The Company of **Biologists**

RESEARCH ARTICLE

C2CD6 regulates targeting and organization of the CatSper calcium channel complex in sperm flagella

Fang Yang[1,*], Maria Gracia Gervasi[2,*], Gerardo Orta[3], Darya A. Tourzani[2], Jose Luis De la Vega-Beltrán[3], Gordon Ruthel[4], Alberto Darszon[3], Pablo E. Visconti[2] and P. Jeremy Wang[1,‡]

ABSTRACT

The CatSper cation channel is essential for sperm capacitation and male fertility. The multi-subunit CatSper complexes form highly organized calcium signaling nanodomains on flagellar membranes. Here, we report identification of an uncharacterized protein, C2CD6, as a subunit of the mouse CatSper complex. C2CD6 contains a calcium-dependent, membrane-targeting C2 domain. C2CD6 associates with the CatSper calcium-selective, core-forming subunits. Deficiency of C2CD6 depletes the CatSper nanodomains from the flagellum and results in male sterility. C2CD6-deficient sperm are defective in hyperactivation and fail to fertilize oocytes both *in vitro* and *in vivo*. CatSper currents are present but at a significantly lower level in C2CD6-deficient sperm. Transient treatments with either Ca^{2+} ionophore, starvation, or a combination of both restore the fertilization capacity of C2CD6-deficient sperm. C2CD6 interacts with EFCAB9, a pH-dependent calcium sensor in the CatSper complex. We postulate that C2CD6 facilitates incorporation of the CatSper complex into the flagellar plasma membrane and may function as a calcium sensor. The identification of C2CD6 may enable the long-sought reconstitution of the CatSper ion channel complex in a heterologous system for male contraceptive development.

KEY WORDS: C2CD6, CatSper, Capacitation, Fertility, Fertilization, Sperm motility, Mouse

INTRODUCTION

Sperm acquires fertilization competence in the female reproductive tract (Chang, 1951). Sperm hyperactivated motility triggered by capacitation is essential for navigation in the oviduct (Suarez, 2016), rheotaxis (Miki and Clapham, 2013) and zona pellucida penetration (Stauss et al., 1995). The uterus and oviduct fluids provide an alkaline environment and a high concentration of bicarbonate, which are essential for capacitation (Vishwakarma, 1962). Sperm motility is regulated by ion channels and ion transporters in the flagellum in response to environmental stimuli (Vyklicka and Lishko, 2020). Calcium influx in sperm is gated by the CatSper ion channel in the flagellum (Ren et al., 2001). The

[1]Department of Biomedical Sciences, University of Pennsylvania School of Veterinary Medicine, Philadelphia, PA 19104, USA. [2]Department of Veterinary and Animal Sciences, University of Massachusetts, Amherst, MA 01003, USA. [3]Departamento de Genética del Desarrollo y Fisiología Molecular, Instituto de Biotecnología, Universidad Nacional Autónoma de México, Cuernavaca, México. [4]Department of Pathobiology, University of Pennsylvania School of Veterinary Medicine, Philadelphia, PA 19104, USA.
*These authors contributed equally to this work

‡Author for correspondence (pwang@vet.upenn.edu)

A.D., 0000-0002-2502-0505; P.J.W., 0000-0003-2311-4089

CatSper channel is activated by alkaline pH in rodents (Kirichok et al., 2006) and primates (Lishko et al., 2010), and by progesterone (P4) in primates (Lishko et al., 2011; Strünker et al., 2011). The CatSper channel forms four linear columns of Ca^{2+} signaling domains along the principal piece of the sperm flagellum (Chung et al., 2014). The CatSper domains organize the spatiotemporal pattern of tyrosine phosphorylation of flagellar proteins, one of the hallmarks of capacitation (Chung et al., 2014; Visconti et al., 1995). Calcium influx caused by CatSper activation results in a powerful, asymmetrical, flagellar-beating movement known as hyperactivation. CatSper is inhibited by efflux of potassium, which is carried out by the Slo3 K^+ channel (KCNU1) (Brenker et al., 2014; Chávez et al., 2014; Geng et al., 2017; Santi et al., 2010; Schreiber et al., 1998; Zeng et al., 2011). In human spermatozoa, P4 binds to its sperm membrane receptor ABHD2, which hydrolyzes the endocannabinoid 2-arachidonoylglycerol (2-AG), an inhibitor of the CatSper channel. As a result, P4 activates CatSper by removing 2-AG from the plasma membrane (Miller et al., 2016). Therefore, sperm hyperactivation is regulated by both environmental stimuli in the female reproductive tract and ion channels on sperm flagella.

The CatSper channel is a complex of ten known subunits: CatSper1-4, CatSperβ, γ, δ, ε, ζ, and EFCAB9 (Lin et al., 2021; Vyklicka and Lishko, 2020; Wang et al., 2021). CatSper1-4 subunits form a heteromeric complex with a central Ca^{2+}-selective pore. The remaining six subunits are auxiliary proteins. CatSperβ, γ, δ and ε are putative transmembrane proteins, whereas CatSperζ and EFCAB9 lack transmembrane domains (Chung et al., 2011, 2017; Hwang et al., 2019; Liu et al., 2007; Wang et al., 2009). Genetic ablation in mice and humans have revealed the role of the CatSper subunits in male fertility. Each of the CatSper core subunits (CatSper1-4) is required for the CatSper complex formation, sperm hyperactivation and, thus, for male fertility (Carlson et al., 2003, 2005; Jin et al., 2007; Qi et al., 2007; Quill et al., 2003; Ren et al., 2001). Like CatSper1-4, CatSperδ is essential for CatSper channel complex assembly and male fertility (Chung et al., 2011). In contrast, CatSperζ- or EFCAB9-deficient males exhibit subfertility (Chung et al., 2017; Hwang et al., 2019). In CatSperζ- or EFCAB9-deficient mouse mutants, the CatSper Ca^{2+} signaling domain organization is affected but the CatSper channel is still functional. EFCAB9 is an EF-hand calcium-binding protein. EFCAB9 interacts with CatSperζ and this interaction requires the binding of Ca^{2+} to EF-hand domains. Thus, EFCAB9, in partnership with CatSperζ, functions as an intracellular pH-dependent Ca^{2+} sensor and activator for the CatSper channel (Hwang et al., 2019). Each of the four columns of CatSper domains consists of two rows. However, in CatSperζ- or EFCAB9-deficient mouse sperm, each column contains only one row of CatSper domains instead of two, suggesting a structural role in addition to their Ca^{2+} sensor function. The CatSper channel is essential for male fertility in humans. Men with loss-of-function

DEVELOPMENT

1

mutations in CatSper subunits are infertile as a result of failures in sperm hyperactivation (Avenarius et al., 2009; Brown et al., 2018; Luo et al., 2019; Smith et al., 2013).

CatSper is probably the most complex ion channel known to date. Despite the extensive genetic, super-resolution structural, and electrophysiological studies, a functional CatSper complex has not been reconstituted in a heterologous system. One possible reason for this is that additional subunits are yet to be identified. Serendipitously, we identified a calcium-binding C2 membrane domain protein (C2CD6) as a previously unknown subunit for the CatSper channel complex. Here, we demonstrate that C2CD6 regulates the targeting and organization of the CatSper complex in mouse sperm flagellar membrane and is essential for sperm hyperactivation and male fertility.

RESULTS
Identification of an evolutionarily conserved sperm flagellar protein

We were interested in interacting proteins of TEX11, a meiosis-specific protein that we previously identified (Yang et al., 2008, 2015). ALS2CR11 was reported as one of the TEX11-interacting proteins in the genome-wide protein-protein interaction study (Rual et al., 2005). However, we find that ALS2CR11 (NP_780409) localizes to sperm flagellum but does not function in meiosis. Because ALS2CR11 contains a calcium-dependent, membrane-targeting C2 domain, it has been renamed as C2CD6 (C2 calcium dependent domain containing 6) (Fig. 1A,B) (Nalefski and Falke, 1996). The *C2cd6* gene is conserved in vertebrates. The transcripts from the *C2cd6* gene locus are very complex. As we were analyzing the *C2cd6* gene structure on chromosome 1, we noticed another uncharacterized gene 3′ downstream, which has a large coding exon (~5 kb), and named it *Als2cr11b* (Fig. 1A). Based on expressed sequence tag profiling, both *C2cd6* and *Als2cr11b* transcripts are testis specific.

We generated polyclonal antibodies against a recombinant C2CD6 N-terminal 386-aa protein. Western blot analysis showed that C2CD6 was present in adult testis but not in ovary or somatic tissues in mice, demonstrating that C2CD6 is testis specific (Fig. 1C). C2CD6 was not detected in epididymis or vas deferens (Fig. S1A). Interestingly, C2CD6 appeared as two major isoforms: C2CD6S (short, ~60 kDa) and C2CD6L (long, ~85 kDa). To determine the nature of these two C2CD6 isoforms, we performed RT-PCR, 3′RACE and sequencing. The presence of two C2CD6 isoforms was due to alternative splicing (Fig. 1A). The *C2cd6s* transcript (GenBank accession number: NM_175200) consists of 13 exons and encodes a protein of 557 aa. The *C2cd6l* transcript (GenBank accession number: MW717645) is more complex and harbors an alternative exon 13, an alternative exon 1 of *Als2cr11b* and splicing of an intron within *Als2cr11b* exon 5. As a result, the protein (691 aa) encoded by the *C2cd6l* transcript is larger than C2CD6S (557 aa) but smaller than ALS2CR11B (1729 aa). C2CD6S and C2CD6L share the first 533 aa and the predicted Ca^{2+}-binding membrane targeting domain (Fig. 1B). Therefore, our C2CD6 antibody recognizes both isoforms. We then generated polyclonal antibodies against the C-terminal 200 aa of ALS2CR11B. Western blot analysis identified a protein band of ~180 kDa in testis but also in lung and brain at a low abundance, suggesting that *Als2cr11b* encodes a bona fide protein (Fig. 1C). Neither C2CD6 nor ALS2CR11B contains predicted transmembrane domains.

We immunostained mouse caudal epididymal sperm with anti-C2CD6 antibodies. Immunofluorescence analysis revealed that C2CD6 localized specifically to the principal piece of sperm flagellum (Fig. 1D), showing that C2CD6 is a component of sperm flagella. The C2CD6 signal is strong at the beginning of the principal piece (at the annulus region) and tapers off towards the end piece. The C2CD6 signal is specific, as it is absent in *C2cd6*-deficient sperm (Fig. 1D). Notably, two distinctive columns of
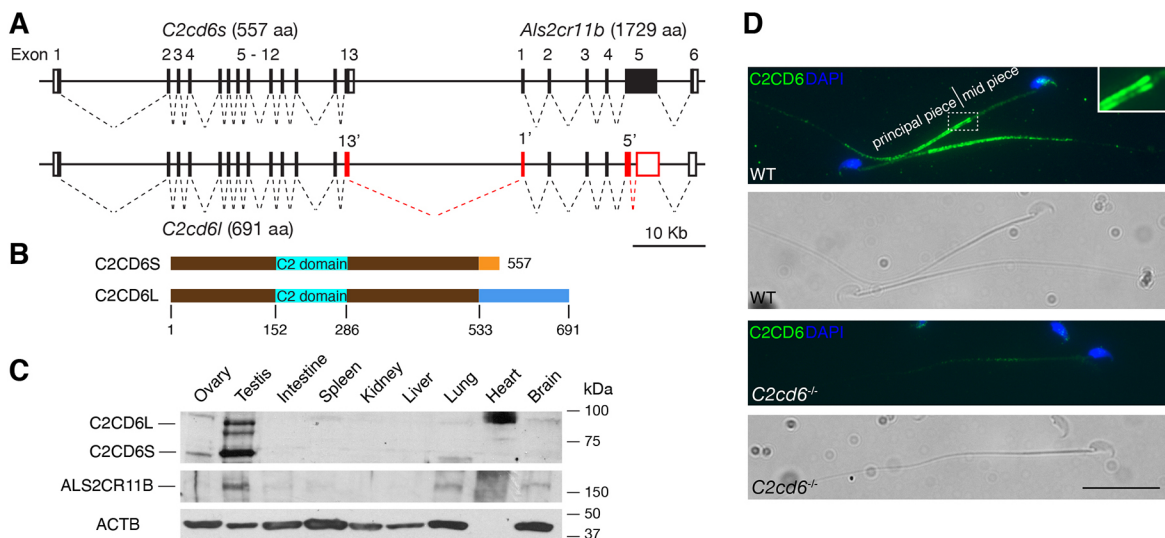

Fig. 1. C2CD6 localizes to the principal piece of sperm flagella. (A) Gene structures of *C2cd6* and *Als2cr11b* on chromosome 1. Coding regions of exons are shown as black boxes. 5′ and 3′ untranslated regions are shown as white boxes. Alternative exons of *C2cd6l* are shown in red. Alternative exons 13′ and 1′ are in-frame. Splicing of an intron within *Als2cr11b* exon 5 results in an early frame shift in the *C2cd6l* transcript. GenBank accession numbers for cDNA sequences: *C2cd6l*, MW717645; *C2cd6s*, NM_175200; *Als2cr11b*, XM_011238634. (B) Schematic of the two C2CD6 protein isoforms C2CD6S and C2CD6L. The N-terminal 533 residues are identical. The Ca^{2+}-binding membrane-targeting C2 domain is predicted based on Phyre2. (C) Western blot analysis of C2CD6 and ALS2CR11B in adult mouse tissues. ACTB serves as a loading control. Note that heart lacks ACTB. (D) C2CD6 localizes to the principal piece of wild-type (WT) mouse sperm but not *C2cd6*-null sperm. Scale bar: 25 µm.

C2CD6 can be observed in the principal piece by widefield fluorescence microscopy (Fig. 1D). We further examined the localization of C2CD6 in testicular and caput epididymal sperm (Fig. S1B). Although C2CD6 was not detected on the growing flagella of step 8 spermatids, C2CD6 was present in the principal piece of the flagella in step 10 testicular sperm and beyond and in caput sperm (Fig. S1B). These results demonstrate that C2CD6 is a component of the sperm flagella.

C2CD6 is essential for male fertility and *in vivo* fertilization

To study the functional requirement of *C2cd6*, we inactivated *C2cd6* by deleting a 1.6-kb genomic region, including exon 1 (containing the initiating codon), through gene targeting in mouse embryonic stem cells (ESCs) (Fig. 2A). Homozygous $C2cd6^{-/-}$ mice were viable and grossly normal. Although $C2cd6^{-/-}$ females had normal fertility, $C2cd6^{-/-}$ males were sterile. $C2cd6^{-/-}$ males produced copulatory plugs, indicating normal mating behavior. Western blotting analysis showed that both C2CD6S and C2CD6L were absent in $C2cd6^{-/-}$ testes, suggesting that the mutant is null (Fig. 2B). Testis weight and sperm count were comparable between $C2cd6^{+/-}$ and $C2cd6^{-/-}$ males (Fig. 2C,D). *C2cd6*-deficient sperm displayed normal morphology. Histology of $C2cd6^{-/-}$ testes showed apparently normal spermatogenesis (data not shown) and thus C2CD6, unlike TEX11 (Yang et al., 2008), is not essential for meiosis.

C2cd6-deficient sperm were apparently motile; however, $C2cd6^{-/-}$ males were sterile. To probe the cause of male infertility, we performed an *in vivo* fertilization test. Wild-type C57BL/6 females were injected with pregnant mare's serum gonadotropin (PMSG) followed by human chorionic gonadotropin (hCG) injection, mated with either $C2cd6^{+/-}$ or $C2cd6^{-/-}$ males (three males per genotype), and copulatory plugs were checked. Twenty-four hours after plug check, eggs/embryos were flushed from oviducts of plugged females. The number of two-cell embryos and one-cell embryos/eggs was counted. The majority of embryos (40/59; 68%) from females plugged by $C2cd6^{+/-}$ males were at the two-cell stage; in contrast, only unfertilized eggs (a total of 51) were obtained from females plugged by $C2cd6^{-/-}$ males (Fig. 2E). These data demonstrate that C2CD6 is required for fertilization *in vivo*.

To determine the capability of *C2cd6*-deficient sperm in egg activation and embryo development, we performed intracytoplasmic sperm injection. Out of 50 oocytes injected with *C2cd6*-deficient sperm, 34 embryos reached the two-cell stage and 20 of them further developed to the blastocyst stage. This result shows that *C2cd6*-deficient sperm can fertilize oocytes by intracytoplasmic sperm injection and support embryo development.

C2CD6 is required for *in vitro* fertilization and hyperactive motility

We next investigated whether *C2cd6*-deficient sperm can fertilize oocytes *in vitro*. We performed *in vitro* fertilization (IVF) assays using cumulus-oocyte complexes from wild-type CD1 females (Table 1). An average fertilization rate of 59% versus 2% was obtained when oocytes were incubated with $C2cd6^{+/-}$ versus *C2cd6*-deficient sperm (Fig. 3A). Only embryos derived from $C2cd6^{+/-}$ sperm developed to blastocysts (76%) after culture in KSOM media (Fig. 3B). The observed 2% fertilization rate obtained with $C2cd6^{-/-}$ sperm was likely due to the low frequency of spontaneous parthenogenetic activation of oocytes (Xu et al., 1997). Therefore, these data indicate that C2CD6 is essential for *in vitro* fertilization.

To determine whether the *in vitro* fertilization failure is related to sperm motility, we performed computer-assisted sperm analysis immediately after sperm swim-out from the epididymis (T0) and after 60 min of incubation under capacitating conditions (T60). No differences in total or progressive sperm motility were found between $C2cd6^{+/-}$ and $C2cd6^{-/-}$ males (Fig. 3C,D). Nevertheless, *C2cd6*-deficient sperm failed to acquire hyperactivated motility after 60 min of incubation under capacitating conditions (Fig. 3E). This could be the cause of the infertility phenotype in $C2cd6^{-/-}$ males, because acquisition of hyperactivated motility is essential for fertilization.

We next evaluated the possibility of restoring fertility of the *C2cd6*-deficient sperm *in vitro*. We applied two sperm treatments prior to IVF that have been proven to restore fertility of other infertile and subfertile mouse models (Navarrete et al., 2016, 2019). Transient treatment with a Ca^{2+} ionophore (ionophore) or sperm energy restriction and recovery (SER) produced a moderate increase
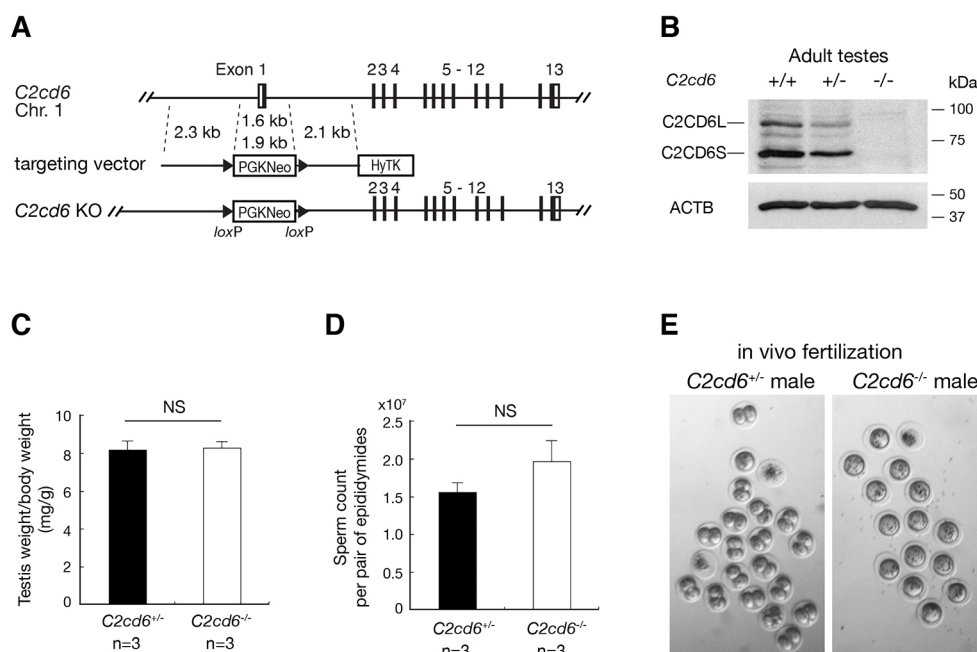

Fig. 2. C2CD6 is essential for *in vivo* fertilization. (A) Targeted inactivation of the *C2cd6* gene. The 1.6-kb deleted region includes exon 1 (containing the initiating start codon) and 600-bp upstream of exon 1 (presumably the promoter region). The neomycin selection marker PGKNeo is flanked by *loxP* sites. HyTK provides negative selection by ganciclovir in ESCs. (B) Western blot analysis of C2CD6 in adult testes. ACTB serves as a loading control. (C) Testis weight normalized to body weight of males at 3-6 months of age. (D) Sperm count of males at 3-6 months of age. NS, not statistically significant (unpaired Student's *t*-test). *n*=3. (E) *In vivo* fertilization assay. Embryos/unfertilized eggs were flushed from wild-type females mated with either $C2cd6^{+/-}$ or $C2cd6^{-/-}$ males.

Table 1. Ionophore and SER treatments

Genotype	Total oocytes	Unfertilized	Degraded	Two-cell embryos	Blastocysts
$C2cd6^{+/-}$ (n=3)	202	95	13	94	74
$C2cd6^{-/-}$ (n=3)	186	168	14	4	0

in the fertilization rates of *C2cd6*-deficient sperm: 6.3% and 18.8%, respectively (Table 2). Strikingly, the combination of SER and ionophore treatments of *C2cd6*-deficient sperm induced an average fertilization rate of 58.8% (Table 2). To analyze embryo development *in vitro*, the obtained two-cell embryos were further cultured in KSOM media. We observed a blastocyst development rate of 22% in the ionophore treatment-derived embryos, 100% in the SER-derived embryos, and 63% in the SER+ionophore-derived embryos. Although each sperm treatment was able to overcome the infertility phenotype of $C2cd6^{-/-}$ males *in vitro*, the combination of SER and ionophore treatments was the most effective.

C2CD6-dependent CatSper organization in sperm flagella

CatSper, the flagellar Ca^{2+} ion channel, localizes to the principal piece (Fig. 4A) (Chung et al., 2017; Ren et al., 2001). C2CD6 localization to the cauda sperm flagella (Fig. 1D) is strikingly similar to CatSper localization. C2CD6 and CatSper1 exhibited similar localization patterns in testicular and caput epididymal sperm (Fig. S1B,C). Moreover, using comparative proteomics,

C2CD6 was shown to be one of the proteins displaying reduced abundance in CatSper1-deficient sperm (Hwang et al., 2019). Therefore, we examined CatSper1 localization in the absence of C2CD6 by immunofluorescence. The CatSper1 signal was severely reduced in $C2cd6^{-/-}$ sperm (Fig. 4A). We also performed super-resolution imaging analysis of CatSper1 and C2CD6 localization in sperm flagellum. As previously reported, CatSper1 formed quadrilateral columns in wild-type flagellum (Fig. 4B). C2CD6 also appeared in columns but was less organized than the CatSper1 columns in wild type (Fig. 4B). In $C2cd6^{-/-}$ sperm, CatSper1 signals were sharply reduced, disorganized, discontinuous, and preferentially distributed to the distal end of the principal piece (Fig. 4A,B).

The CatSper complex is partitioned into microsomes (vesicle-like structures formed from pieces of endoplasmic reticulum) in testis extracts (Chung et al., 2017). We prepared microsomes from wild-type and $C2cd6^{-/-}$ testes (Fig. 4C). C2CD6, like CatSper1, was present in testicular microsome fractions. In addition, CatSper1 was abundant in microsome fractions from $C2cd6^{-/-}$ testes (Fig. 4C), suggesting that synthesis of CatSper is not affected in $C2cd6^{-/-}$
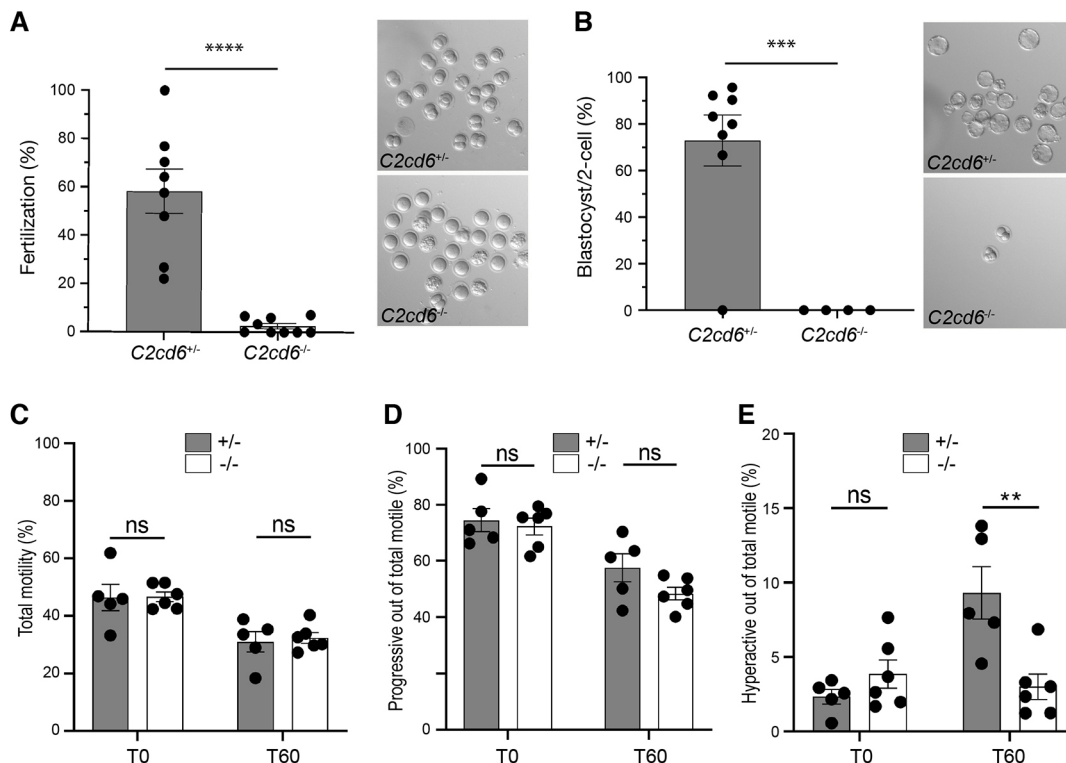

Fig. 3. C2CD6 is required for *in vitro* fertilization and sperm hyperactivation. (A) *In vitro* fertilization. CD1 cumulus-oocyte complexes were incubated with $C2cd6^{+/-}$ or $C2cd6^{-/-}$ sperm. Fertilization rate is the percentage of oocytes inseminated that develop into two-cell embryos after 24 h of incubation. A representative image for each treatment is shown. ****$P<0.0001$. (B) Percentage of two-cell embryos that develop to the blastocyst stage after culture in KSOM media. A representative image for each treatment is shown. ***$P<0.001$. (C) Percentage of motile sperm immediately after swim-out in TYH medium (T0) and after 60 min of incubation in capacitating conditions in TYH medium (T60). Sperm motility was analyzed by computer-assisted sperm analysis. (D) Percentage of the motile sperm displaying progressive motility at T0 and at T60 of incubation in capacitating conditions. (E) Percentage of the motile sperm displaying hyperactive motility at T0 and at T60 of incubation in capacitating conditions. ns, not statistically significant, **$P<0.01$. Unpaired Student's *t*-tests were performed for statistical analysis. n=5 or 6.

Table 2. *In vitro* fertilization

	Genotype	Control	Ionophore (20 µM)	SER	SER+ionophore (5 µM)
Fertilization (%)	$C2cd6^{+/-}$	222/405 (54.8)	46/48 (95.8)	–	–
	$C2cd6^{-/-}$	10/389 (2.6)	6/96 (6.3)	15/80 (18.8)	50/85 (58.8)
Blastocyst/two-cell (%)	$C2cd6^{+/-}$	144/222 (64.9)	43/46 (93.5)	–	–
	$C2cd6^{-/-}$	0/10 (0)	2/5 (22.2)	14/14 (100)	31/50 (62.7)

testes. We next performed western blotting analysis of sperm extracts. As expected, both C2CD6 and CatSper1 were present in wild-type and $C2cd6^{+/-}$ sperm extracts (Fig. 4D). However, CatSper1 abundance was dramatically reduced in $C2cd6^{-/-}$ sperm extract (Fig. 4D). Taken together, our results demonstrate that CatSper1 is abundant in the testis but fails to become incorporated into sperm flagella fully or efficiently in the absence of C2CD6.

We next sought to address whether CatSper is required for C2CD6 localization. Both CatSper1 and C2CD6 were detected in $CatSper1^{+/+}$ testis microsome extract (Fig. 4E). C2CD6 was present in $CatSper1^{-/-}$ testis microsome extract and its abundance was comparable to that in $CatSper1^{+/-}$ testis (Fig. 4E). As expected, CatSper1 was absent in $CatSper1^{-/-}$ flagellum (Fig. 4F). C2CD6 was sharply reduced in $CatSper1^{-/-}$ flagellum (Fig. 4G). This result is consistent with the reduced abundance of C2CD6 in $CatSper1^{-/-}$ sperm shown by quantitative proteomic analysis (Hwang et al., 2019). These results demonstrate that CatSper is required for C2CD6 localization in sperm flagella. Therefore, the inter-dependent localization of C2CD6 and CatSper1 suggests that C2CD6 might be an important component of the CatSper complex.

CatSper is functional but at a substantially reduced capacity in *C2cd6*-deficient sperm

To investigate whether the CatSper channel is functionally assembled in $C2cd6$-deficient sperm, we recorded the CatSper current ($I_{CatSper}$) using whole-cell patch-clamp measurements in cauda sperm (Kirichok et al., 2006; Orta et al., 2018). Both inward and outward $I_{CatSper}$ currents recorded from $C2cd6^{-/-}$ sperm were a fraction (17% and 26%, respectively) of the currents from $C2cd6^{+/-}$ sperm (Fig. 5A). The $I_{CatSper}$ in sperm from both $C2cd6^{+/-}$ and $C2cd6^{-/-}$ mice was stimulated by alkalinization induced by addition of 10 mM NH_4Cl to the bath solution (Fig. 5B,C). In conclusion, though reduced in magnitude, $I_{CatSper}$ from $C2cd6^{-/-}$ sperm showed voltage- and alkali-induced activation, properties that are characteristic of CatSper.

Calcium influx regulates protein kinase A (PKA) phosphorylation and protein tyrosine phosphorylation in sperm upon capacitation. The phosphorylation of PKA substrates was diminished in sperm from $C2cd6^{-/-}$ males in comparison with $C2cd6^{+/-}$ males (Fig. S2A). However, the increase in tyrosine phosphorylation that occurs during sperm capacitation was similar in $C2cd6^{-/-}$ sperm and $C2cd6^{+/-}$ sperm (Fig. S2B). These results are consistent with the biphasic
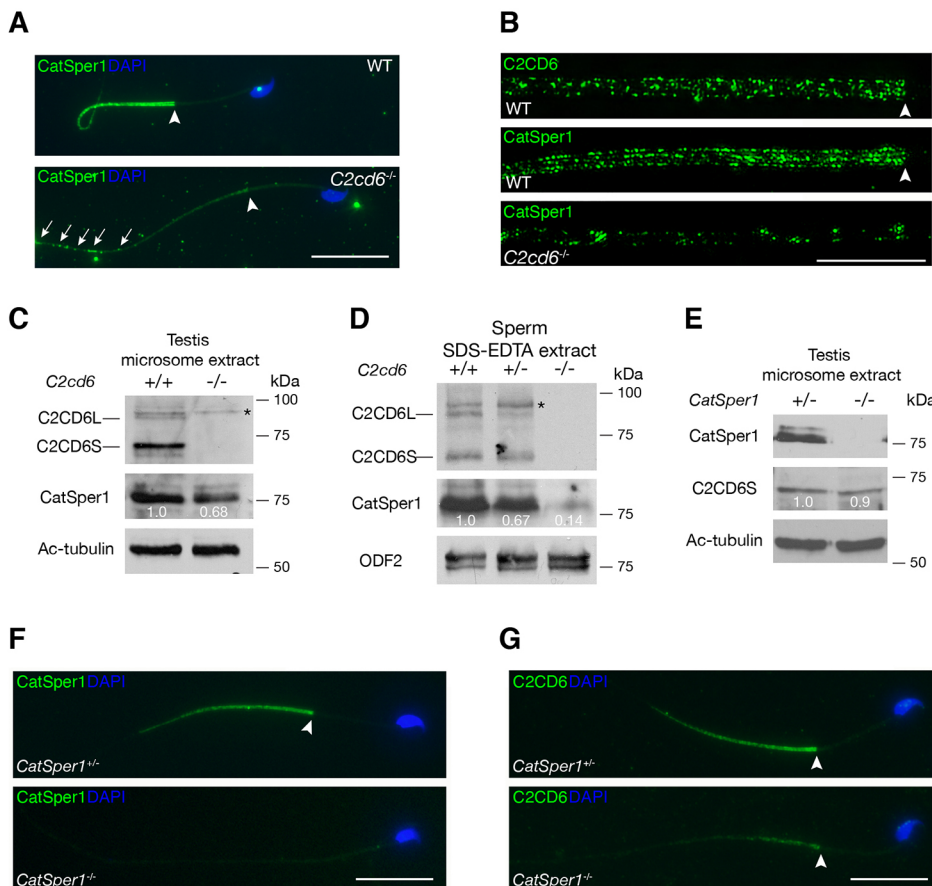

Fig. 4. C2CD6 regulates targeting and nanodomain organization of CatSper in sperm flagella. (A) Immunofluorescence analysis of CatSper1 in wild-type (WT) and *C2cd6*-deficient sperm. Arrowheads indicate the annulus. (B) Super-resolution localization of C2CD6 and CatSper1 in wild-type and $C2cd6^{-/-}$ sperm. The distal region of the flagellar principal piece of the $C2cd6^{-/-}$ sperm is shown. (C) Western blot analysis of C2CD6 and CatSper1 in testis microsome fractions from adult wild-type and $C2cd6^{-/-}$ males. Acetylated tubulin (Ac-tubulin) serves as a loading control. (D) Western blot analysis of C2CD6 and CatSper1 in sperm extracts from adult wild-type, $C2cd6^{+/-}$ and $C2cd6^{-/-}$ males. ODF2, a component of flagellar outer dense fibers, serves as a loading control (Cao et al., 2006). (E) Western blot analysis of CatSper1 and C2CD6 in microsome extracts from adult $CatSper1^{+/-}$ and $CatSper1^{-/-}$ testes. In C-E, western blot band intensity was normalized to Ac-tubulin or ODF2. Relative band intensity is shown. (F) Immunofluorescence analysis of CatSper1 in $CatSper1^{+/-}$ and $CatSper1^{-/-}$ sperm from 3- to 6-month-old males. (G) Immunofluorescence analysis of C2CD6 in $CatSper1^{+/-}$ and $CatSper1^{-/-}$ sperm from 3- to 6-month-old adult males. Additional fluorescence images are provided in Fig. S3. Scale bars: 25 µm (A,F,G); 5 µm (B).
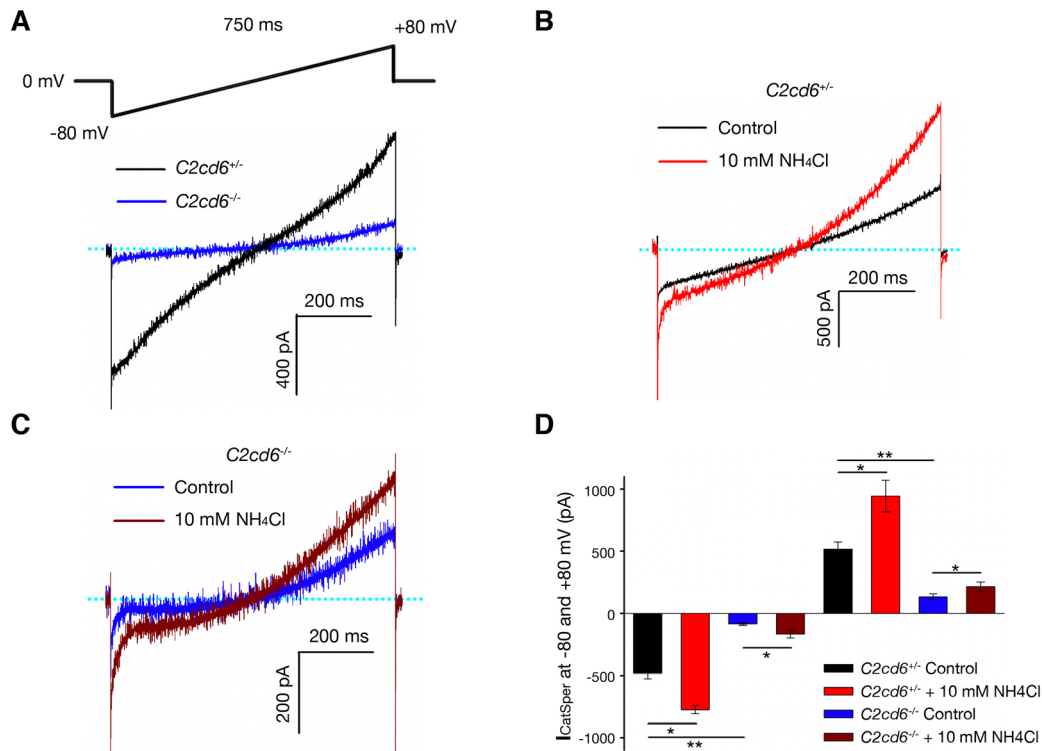
Fig. 5. The CatSper channel is functional but at a significantly reduced capacity in $C2cd6^{-/-}$ cauda sperm. (A) Representative CatSper currents in cauda sperm from adult $C2cd6^{+/-}$ and $C2cd6^{-/-}$ mice. (B) CatSper currents in $C2cd6^{+/-}$ cauda sperm before (control) and after alkalization with 10 mM NH_4Cl. (C) CatSper currents in $C2cd6^{-/-}$ cauda sperm before (control) and after alkalization with 10 mM NH_4Cl. (D) Average CatSper currents in cauda sperm measured at -80 mV and $+80$ mV. The experiments were performed on cauda sperm from four $C2cd6^{+/-}$ and four $C2cd6^{-/-}$ mice at 3-6 months of age. *$P<0.05$, **$P<0.01$ (paired Student's t-test). $n=4$.

action of Ca^{2+} in the regulation of cAMP-dependent pathways as previously reported (Navarrete et al., 2015).

Previously, it was reported that addition of bovine serum albumin (BSA) to sperm induced an increase in intracellular Ca^{2+} concentration, $[Ca^{2+}]i$ (Xia and Ren, 2009). Here, we compared the BSA-induced $[Ca^{2+}]i$ increase in $C2cd6^{+/-}$ and $C2cd6^{-/-}$ sperm. Addition of BSA (5 mg/ml) reproducibly increased $[Ca^{2+}]i$ in the $C2cd6^{+/-}$ sperm; however, this response was substantially smaller in the $C2cd6^{-/-}$ sperm (Fig. S4A,B). Quantification of the normalized BSA responses with respect to ionomycin showed a significantly lower response in $C2cd6^{-/-}$ sperm than in $C2cd6^{+/-}$ sperm (Fig. S4C). Taken together, these results indicate that functional CatSper channels are assembled in the absence of C2CD6 but substantially reduced in capacity (Fig. 5D).

Association of C2CD6 with components of the CatSper complex

The CatSper complex from sperm protein extracts is not soluble, preventing co-immunoprecipitation analysis of this complex using such protein extracts. To investigate the connection of C2CD6 with the CatSper channel complex, we co-expressed C2CD6 with CatSper complex components in HEK293T cells and tested their interaction by co-immunoprecipitation. C2CD6 and all CatSper components are expressed in testis but are absent in somatic cells such as HEK293T cells. The abundance of C2CD6 in transfected HEK293T cells was low but dramatically enriched by immunoprecipitation (Fig. 6). The full-length C2CD6 migrated at 75 kDa and a slightly smaller isoform was also present in the immunoprecipitated fraction (Fig. 6A). CatSper1 was present in the C2CD6 complex (Fig. 6A). CatSper2 was also in complex with

C2CD6 but the association was weak (Fig. 6B). CatSper3 was strongly associated with C2CD6 (Fig. 6C). CatSper4 was readily detected in C2CD6-immunoprecipated proteins, indicating a strong association between CatSper4 and C2CD6 (Fig. 6D). EFCAB9 was abundant in C2CD6-immunoprecipated proteins, showing that EFCAB9 is strongly associated with C2CD6 (Fig. 6E). However, we did not detect association between C2CD6 and CatSperz (TEX40) (Fig. 6F). Collectively, C2CD6 associates with the core components of the CatSper complex (Fig. 6G).

DISCUSSION

Here, we demonstrate that C2CD6 associates with the CatSper complex and regulates its localization and function. Our study strongly suggests that in addition to the ten known subunits, C2CD6 is a previously unidentified subunit of the CatSper complex (Fig. 6G). Four core α subunits, CatSper1-4, form the membrane-spanning Ca^{2+}-selective pore. C2CD6 associates with all four α subunits, suggesting that it may directly bind to the CatSper channel core. In addition, C2CD6 associates with EFCAB9 but not with CatSperz, a partner of EFCAB9. We postulate that C2CD6 plays an important role in the CatSper nanodomain organization in sperm flagella. C2CD6 contains a calcium-dependent, membrane-targeting C2 domain. This domain is found in signaling proteins that interact with the cellular membrane (Nalefski and Falke, 1996). This raises the possibility that C2CD6 might facilitate targeting of assembled CatSper complexes to the sperm flagellar plasma membrane or insertion into the membrane. Indeed, CatSper1 is present in testis but its abundance is substantially reduced in sperm from $C2cd6^{-/-}$ males and displays disrupted quadrilateral domain localization in the
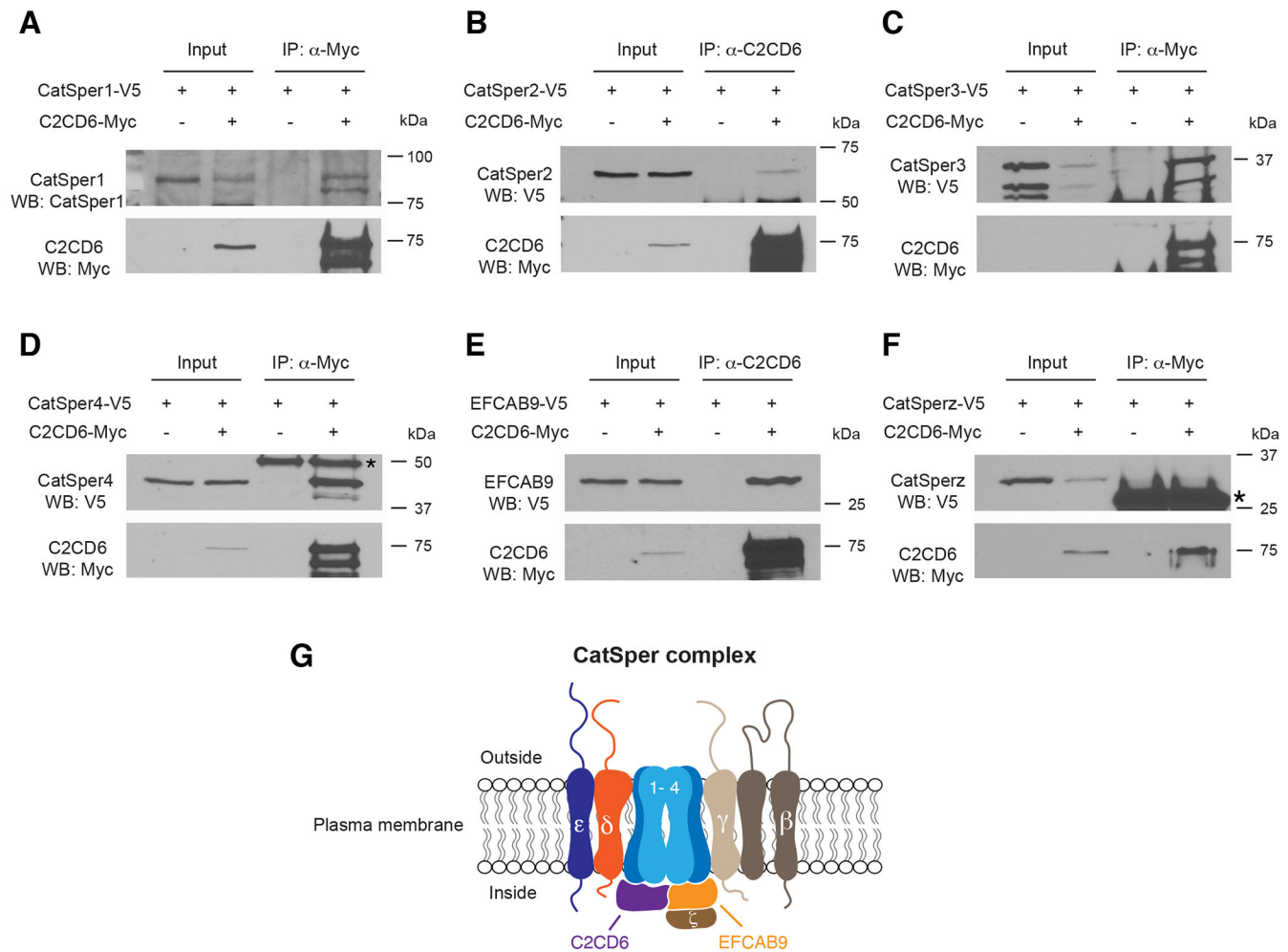
Fig. 6. C2CD6 associates with subunits of the CatSper channel complex. (A-F) HEK293T cells were transfected with the indicated expression constructs and protein extracts were used for immunoprecipitation (IP) and western blotting (WB) analyses. Input is 1% of the protein extracts used for IP. The antibodies used for IP and WB are shown in each panel. Co-immunoprecipitation of C2CD6 with CatSper1 (A), CatSper2 (B), CatSper3 (C), CatSper4 (D) and EFCAB9 (E) was demonstrated. Asterisk in D indicates Ig heavy chain. (F) C2CD6 is not associated with CatSperz. Asterisk indicates Ig light chain. (G) A working model of the CatSper channel complex. Eleven known subunits of the CatSper channel, including C2CD6, are shown. C2CD6 is associated with CatSper 1-4 and EFCAB9.

principal piece. Consistently, the CatSper current is still present in *C2cd6*-deficient sperm, although it is dramatically reduced. These results indicate that the CatSper complex is not efficiently targeted to the sperm flagella without C2CD6. These C2CD6 results are in stark contrast with the removal of each of the CatSper core subunits. In each of these cases, the remaining subunits are expressed in the testes but are absent in mature sperm (Qi et al., 2007). The presence of the residual CatSper complex in C2CD6-null sperm flagella supports the suggestion that C2CD6 is the main protein for CatSper transport and targeting but other unknown proteins also play a minor role. In addition, C2CD6 might function as a Ca^{2+} sensor for CatSper independently or as a complex with EFCAB9. Notably, the CatSper channel is compromised but still conducts currents in EFCAB9-deficient sperm (Hwang et al., 2019). In EFCAB9-deficient sperm, C2CD6 might be responsible for Ca^{2+} sensing. Our results are consistent with a preprint independent study by Hwang et al. (2021).

The cryo-electron microscopic structure of the CatSper channel complex (termed CatSpermasome) has been reported (Lin et al., 2021). Mass spectrometric analysis of the CatSpermasome revealed the presence of C2CD6 in the complex (Lin et al., 2021). However,

C2CD6 was not delineated in the structure of this complex. There are several unsolved extra densities in the structure, which likely include C2CD6 and other uncharacterized components. Our *in vitro* association results (Fig. 6) indicate that C2CD6 may belong to the unsigned cytosolic region map 1 (Lin et al., 2021). CDC42 localizes to four linear domains in sperm flagella and its localization is disrupted in CatSper1-null sperm (Luque et al., 2021). However, CDC42 is absent in the CatSpermasome (Lin et al., 2021), suggesting complexity in the regulation of the CatSper ion channel activity.

C2CD6 exists as at least two isoforms. Both isoforms contain the C2 domain and are present in sperm. It is not known whether these two isoforms are functionally redundant or have isoform-specific functions. Intriguingly, CatSperδ also has two isoforms resulting from alternative splicing (Chung et al., 2011). In addition, C2CD6 is tyrosine phosphorylated upon capacitation (Chung et al., 2014). The physiological consequence of this phosphorylation on C2CD6 is unknown. The *Als2cr11b* gene encodes a bona fide protein in testis (Fig. 1C). Like *C2cd6*, *Als2cr11b* is conserved in vertebrates. Future study is necessary to investigate whether ALS2CR11B is a subunit of the CatSper complex. Genetic ablation of *Als2cr11b* alone

DEVELOPMENT

7

without disruption of *C2cd6* is challenging, because *Als2cr11b* shares exons with *C2cd6l* (Fig. 1A).

C2cd6⁻/⁻ sperm do not fertilize oocytes *in vivo* or *in vitro*. The sterility phenotype is caused by a failure to induce hyperactivated motility during sperm capacitation. Hyperactivated motility is characterized by a high-amplitude asymmetrical beating of the sperm flagellum (Suárez and Osman, 1987). This flagellar beating pattern is mainly regulated by $[Ca^{2+}]_i$, which is maintained by ion channels and pumps in the plasma membrane (Visconti et al., 2011). Two of the most important sperm $[Ca^{2+}]_i$ regulators are the CatSper channel, which is essential for the entrance of Ca^{2+} into sperm (Ren et al., 2001), and the Ca^{2+} efflux pump PMCA4 (ATP2B4), which is required for Ca^{2+} clearance (Wennemuth et al., 2003). The proper assembly and function of the CatSper channel are essential for acquisition of sperm hyperactivated motility and fertility (Chung et al., 2011, 2017; Hwang et al., 2019; Ren et al., 2001). Consistent with our conclusion that C2CD6 is a subunit of the CatSper channel complex, *C2cd6*-deficient sperm fail to achieve hyperactivated motility after incubation under capacitating conditions.

Ca^{2+} is a second messenger with pivotal roles in activating (or inhibiting) downstream effectors during sperm capacitation (Navarrete et al., 2015). The transient treatment of sperm with the Ca^{2+} ionophore A23187 can bypass the activation of the main molecular pathway involved in acquisition of fertilizing capacity during sperm capacitation: the cAMP/PKA pathway (Tateno et al., 2013). This transient sperm ionophore treatment was applied prior to IVF and successfully reversed the male sterility phenotype of *CatSper1⁻/⁻*, *sAC⁻/⁻* and *Slo3⁻/⁻* mice as moderate fertilization was achieved (Navarrete et al., 2016). In line with these previous observations, the ionophore treatment prior to IVF in *C2cd6*-deficient sperm reversed the sterility phenotype, indicating that an increase of intracellular Ca^{2+} is sufficient to restore fertility in this mouse model. We have recently developed another sperm treatment that improves fertilization rates and embryo development of sub-fertile mouse models by manipulation of the sperm metabolism (Navarrete et al., 2019). When applied prior to IVF in *CatSper1⁻/⁻* sperm, this SER treatment was not able to restore fertility; however, a combination of the ionophore A23187 and the SER treatments induced a synergistic effect on fertilization rates and embryo development in the *CatSper1⁻/⁻* model (Navarrete et al., 2019). The same synergistic effect was observed on *C2cd6*-deficient sperm. Interestingly, although the SER treatment did not rescue the sterility phenotype of *CatSper1⁻/⁻* mice (Navarrete et al., 2019), the application of SER treatment alone was able to overcome the sterility phenotype of the *C2cd6⁻/⁻* mice. This could be related to our recent findings that SER treatment induces an elevation of $[Ca^{2+}]_i$ in mouse sperm from wild-type and *CatSper1⁻/⁻* animals (Sánchez–Cárdenas et al., 2021). It could also be due to the presence of residual functional CatSper channels in *C2cd6*-deficient sperm. Another possible explanation for the difference in the SER treatment response is that C2CD6 could regulate capacitation independently of CatSper.

The CatSper channel is essential for sperm hyperactivation and male fertility in both mice and humans. The CatSper subunits are only expressed in testis and sperm. Traditionally, ion channels are druggable targets. For these reasons, the CatSper channel has been proposed as a target for male contraception with minimal side effects. However, reconstitution of CatSper in a heterologous system has not been achieved, despite the fact that CatSper was discovered two decades ago (Ren et al., 2001). The lack of a heterologous system impedes drug discovery efforts for small molecule inhibitors of CatSper. The challenges for developing a

CatSper heterologous system are several fold. First, the CatSper ion channel is extremely complex. It is still possible that not all CatSper-associated proteins are known. Second, the CatSper assembly might require chaperones. The CatSper complex is associated with a testis-specific chaperone, HSPA2 (Chung et al., 2011; Zhu et al., 1997). Third, sperm flagellum is a unique ciliary structure. CatSper forms organized linear domains along the principal piece. Organization of these nanodomains might depend on other flagellar unique structures, such as the fibrous sheath, which is absent in heterologous cells. The identification of C2CD6 might facilitate successful development of a heterologous CatSper system, which is not only crucial for drug development but would also provide an amenable system in which to dissect the mechanistic role of each subunit in CatSper.

MATERIALS AND METHODS
Generation of *C2cd6* knockout mice
The targeting strategy was to delete a 1.6-kb genomic region including exon 1 of the *C2cd6* gene (Fig. 2A). In the targeting construct, the left (2.3 kb) and right (2.1 kb) homologous arms were PCR amplified from a *C2cd6*-containing mouse BAC clone (RP24-535E21) with high-fidelity Taq DNA polymerase. A neomycin (PGKNeo) selection marker was inserted between the homologous arms. The HyTK selection marker was cloned adjacent to the right arm. V6.5 ESCs were electroporated with the ClaI-linearized targeting construct and cultured in the presence of 350 μg/ml G418 and 2 μM ganciclovir. ESC clones were screened by long-distance PCR for homologous recombination. Out of 192 ESC clones, nine homologously targeted clones were identified. 2C5 and 1H1 ESC clones were injected into blastocysts and the resulting chimeric mice transmitted the *C2cd6* knockout allele through the germline. The *C2cd6⁺/⁻* 2C5 mice were backcrossed to the C57BL/6J strain four times (N4). All the experiments were performed on the C57BL/6J N4 backcrossed mice. Mice were genotyped by PCR of tail genomic DNA with the following primers: wild type (515 bp), ALS-25 (5′-GTATTTCCCATCATGTGGAGGA-3′) and ALS-26 (5′-AGTGGCTTGCCTTCTTCATCAG-3′); *C2cd6* knockout allele (341 bp), ALS-9 (5′-TGTGCTATCCACCTTGCCTT-3′) and PGKRNrev2 (5′-CCTACCGGTGGATGTGGAATGTGTG-3′).

CatSper1 knockout mice were previously generated (Ren et al., 2001).

All experiments with mice were performed in accordance with the Institutional Animal Care and Use Committee (IACUC) guidelines of the University of Pennsylvania and the University of Massachusetts at Amherst.

Antibody production
The *C2cd6* cDNA was amplified from bulk mouse testis cDNA by PCR. The cDNA fragment encoding residues 1-386 was cloned into the pQE-30 vector (QIAGEN). The 6×His-C2CD6 (aa 1-386) fusion protein was expressed in M15 bacteria, affinity purified with Ni-NTA beads, and eluted in 8 M urea. The recombinant fusion protein was used to immunize two rabbits at Cocalico Biologicals. The C2CD6 antiserum (UP2429 and UP2430) was used for western blotting analysis (1:500). Specific antibodies for immunofluorescence were affinity purified with the immunoblot method (Harlow and Lane, 1998). The specificity of the C2CD6 antibody was validated by western blotting and by immunofluorescence analyses in testes and sperm from C2CD6-deficient mice.

The *Als2cr11b* cDNA fragment encoding the C-terminal 200 residues was cloned into the pQE-30 vector. The 6× His-ALS2CR11B (C-terminal 200 aa) fusion protein was expressed in bacteria, affinity purified, and used to immunize two rabbits at Cocalico Biologicals, resulting in one anti-ALS2CR11B antiserum (UP2443).

In vivo fertilization
Eight-week-old wild-type C57BL/6 females were injected with 7.5 IU of PMSG, then with 7.5 IU of hCG 46 h later, and mated with either *C2cd6⁺/⁻* or *C2cd6⁻/⁻* males. Copulatory plugs were checked 17 h after mating setup. Twenty-four hours after plug check, eggs/embryos were flushed from plugged females. The numbers of two-cell embryos and one-cell embryos/eggs were counted.

Sperm collection

Cauda epididymides from 3-month-old males were dissected and placed in Toyoda–Yokoyama–Hosi (TYH) medium containing 119.37 mM NaCl, 4.7 mM KCl, 1.71 mM CaCl$_2$, 1.2 mM KH$_2$PO$_4$, 1.2 mM MgSO$_4$, 25.1 mM NaHCO$_3$, 0.51 mM sodium pyruvate, 5.56 mM glucose, 4 mg/ml BSA, 10 μg/ml gentamicin and 0.0006% Phenol Red equilibrated in 5% CO$_2$ at 37°C. After 10 min of sperm swim-out, epididymal tissue was removed and sperm suspensions were further incubated in TYH medium in 5% CO$_2$ at 37°C to allow sperm to capacitate.

Sperm motility analysis

Sperm motility parameters were analyzed immediately after swim-out (T0) and after 60 min (T60) of incubation in capacitating conditions (TYH medium). Sperm suspensions were loaded onto 100-μm-depth chamber slides (Leja, Spectrum Technologies), placed in a slide warmer at 37°C (Minitherm, Hamilton Thorne), and imaged with a 4× dark field objective (Olympus) on a Lab A1 microscope (Zeiss). Ninety frame videos were recorded at 60 Hz and analyzed using a CEROS II computer-assisted sperm analysis system (Hamilton Thorne). The settings for cell recognition included: head size, 5-200; minimum head brightness, 100; and static head elongation, 5-100%. Sperm with average path velocity (VAP)>0 and rectilinear velocity (VSL)>0 were considered motile. Sperm were considered progressive with VAP>50 μm/s and straightness (STR)>50%, and hyperactive with curvilinear velocity (VCL)>271 μm/s, VSL/VCL (LIN)<50%, and amplitude of lateral head displacement (ALH)>3.5 μm. At least five fields per treatment corresponding to a minimum of 200 sperm were analyzed per experiment. Data were presented as the percentage of motile sperm out of the total population, and percentage of progressive or hyperactive sperm out of the motile population.

IVF

Young (7- to 9-week-old) CD-1 females were obtained from Charles River Laboratories. Superovulation was induced by injection first with 7.5 IU of PMSG (493-10, Lee Biosolutions), followed 48 h later with 7.5 IU of hCG (CG5, Sigma-Aldrich). Females were sacrificed 13 h post-hCG injection, the oviducts were dissected, and cumulus-oocyte complexes (COCs) were collected in TL-HEPES medium containing 114 mM NaCl, 3.22 mM KCl, 2.04 mM CaCl$_2$, 0.35 mM NaH$_2$PO$_4$, 0.49 mM MgCl$_2$, 2.02 mM NaHCO$_3$, 10 mM lactic acid (sodium salt) and 10.1 mM HEPES. COCs were thoroughly washed with TYH medium and placed in an insemination drop of TYH medium covered by mineral oil previously equilibrated in an incubator in 5% CO$_2$ at 37°C. COCs (two or three per 90 μl drop) were inseminated with 100,000 sperm that were previously capacitated in TYH medium for 60 min, and then were maintained in an incubator in 5% CO$_2$ at 37°C. After 4 h of insemination, the MII-oocytes were washed, placed in a different drop of TYH media, and incubated overnight in 5% CO$_2$ at 37°C. Dishes were examined 24 h post-insemination, and fertilization was evaluated by the appearance of two-cell-stage embryos. Results were expressed as percentage of two-cell embryos out of the total number of oocytes inseminated.

Enhanced IVF

SER and Ca^{2+} ionophore treatments prior to IVF improve the rate of fertilization in subfertile and infertile animals (Navarrete et al., 2016; Navarrete et al., 2019). The following sperm treatments prior to IVF were tested: (1) control (TYH); (2) control+Ca^{2+} ionophore; (3) SER; and (4) SER+Ca^{2+} ionophore. For each 3-month-old male, one cauda epididymis was collected and placed in TYH medium (tube A) and the other cauda epididymis was collected and placed in TYH medium devoid of glucose and pyruvate (SER-TYH, tube B). After 10 min of incubation in 5% CO$_2$ at 37°C to allow sperm swim-out, cauda tissues were removed. Sperm suspensions were centrifuged twice at 150 *g* for 5 min and the sperm pellet was washed with 2 ml of TYH for tube A and 2 ml of SER-TYH for tube B. After the final wash, sperm pellets were resuspended in 500 μl of TYH for tube A and 500 μl of SER-TYH for tube B. Each tube was immediately divided into two 250 μl suspensions and incubated in 5% CO$_2$ at 37°C until the sperm motility from treatments 3 and 4 was significantly slow (about 30 min). At that point, the Ca^{2+} ionophore 4Br-A23187 (C7522, Fisher

Scientific) was added to a final concentration of 20 μM for treatment 2 and 5 μM for treatment 4. When used in combination with the SER treatment, 20 μM ionophore was detrimental to the sperm sample and, therefore, the concentration of ionophore was decreased to 5 μM for treatment 4. After a 10-min incubation with Ca^{2+} ionophore, 1.5 ml of TYH was added to all the treatments followed immediately by centrifugation at 150 *g* for 5 min. Sperm pellets were then washed again with TYH and centrifuged at 150 *g* for 5 min. Sperm pellets were resuspended in 500 μl of TYH and used for insemination of COCs. All the procedures after insemination were performed as described above for regular IVF.

Embryo culture

The two-cell embryos from IVF were washed and placed in a dish of equilibrated KSOM media (MR-106-D, Fisher Scientific) covered by light mineral oil (0121-1, Fisher Scientific). Embryo culture dishes were incubated for 3.5 days in 5% CO$_2$, 5% O$_2$, at 37°C. Results are expressed as the percentage of blastocysts out of the total number of two-cell embryos and the percentage of blastocysts out of the total number of oocytes inseminated.

Immunofluorescence and super-resolution imaging

After three incisions, cauda epididymides were incubated in PBS at 37°C for 10 min. For testicular spermatids or caput sperm, seminiferous tubules or caput epididymis were squeezed to obtain sperm suspensions. Swim-out sperm or sperm cell suspensions were placed on slides and fixed in 2% paraformaldehyde in PBS with 0.2% Triton X-100 overnight. The slides were incubated with rabbit anti-C2CD6 (UP2430, 1:100) or rabbit anti-Catsper1 (1:200) antibodies and/or mouse anti-acetylated tubulin (T7451, 1:200, Sigma), then with anti-rabbit FITC-conjugated secondary antibody (1:100, FI-1000, Vector Laboratories) and/or anti-mouse Texas Red-conjugated secondary antibody (1:100, TI-2000, Vector Laboratories), and then mounted with DAPI. Images were captured with an ORCA digital camera (Hamamatsu Photonics) on a Leica DM5500B microscope. For structured illumination microscopy imaging, images were acquired on a GE DeltaVision OMX SR imaging system with PCO sCMOS cameras and were processed using Softworx software.

Testis microsome extraction

One adult testis (~100 mg) was homogenized on ice in 1 ml 0.32 M sucrose solution with 1× protease inhibitor cocktail (P8340, Sigma-Aldrich). After centrifugation at 300 *g* at 4°C for 10 min, the supernatant was transferred to an ultra-centrifuge tube and centrifuged at 100,000 *g* for 1 h. The pellet containing the microsome fraction was resuspended and solubilized in 5 ml PBS with 1% Triton X-100 and 1× protease inhibitor cocktail by rocking at 4°C for 2 h. The suspension was centrifuged at 15,000 *g* for 30 min and the supernatant was collected for western blot analysis.

Sperm protein extraction

Sperm (~1.3×10^7) were collected from one adult mouse by squeezing the cauda epididymides in PBS solution followed by centrifugation at 800 *g* for 5 min at room temperature. Sperm were homogenized in 100 μl SDS-EDTA solution (1% SDS, 75 mM NaCl, 24 mM EDTA, pH 6.0) and centrifuged at 5000 *g* for 30 min at room temperature, and then 100 μl 2× SDS-PAGE sample buffer (62.5 mM Tris, pH 6.8, 3% SDS, 10% glycerol, 5% β-mercaptoethanol, 0.02% Bromophenol Blue) was added to 100 μl of supernatant. The samples were heated at 95°C for 10 min and 20 μl of each sample (equivalent to 1.3×10^6 sperm) was used for western blot analysis.

Electrophysiology

In brief, cauda epididymal sperm were obtained by swim-out in TYH medium (Orta et al., 2018) and stored in HS buffer: 135 mM NaCl, 5 mM KCl, 2 mM CaCl$_2$, 1 mM MgSO$_4$, 10 mM lactic acid, 1 mM pyruvic acid, 5 mM glucose, 20 mM HEPES, pH 7.4. For the CatSper current (I_CatSper) recording, we used a divalent cation-free solution (DVF) (150 mM Na-gluconate, 2 mM Na$_2$EDTA, 2 mM EGTA, 20 mM HEPES, pH 7.4) (Kirichok et al., 2006; Orta et al., 2018). The intrapipette solution contained 135 mM Cs-MeSO$_3$, 5 mM CsCl, 10 mM EGTA, 20 mM HEPES, pH 7.2. Whole-cell I_CatSper was obtained by patch clamping the sperm cytoplasmic

droplet (Orta et al., 2018). Seals (>5 GΩ) between the patch pipette and the cytoplasmic droplet in sperm were formed in HS bath solution, and, after achieving whole-cell configuration, the bath solution was changed to DVF solution. $I_{CatSper}$ was induced by applying a voltage-ramp protocol from −80 mV to +80 mV with a 750 ms time duration from a holding potential of 0 mV. For alkinization, 10 mM NH_4Cl was added to the bath solution. The $I_{CatSper}$ data were analyzed using Clampfit 10.7 (Molecular Devices) and were plotted with SigmaPlot 10.0 (Systat Software). Data are shown as mean ±s.e.m. (Fig. 5D). Differences between treatments (without versus with NH_4Cl) were analyzed by paired Student's t-test. Differences between genotypes ($C2cd6^{+/−}$ vs $C2cd6^{−/−}$) were tested by unpaired Student's t-test. Differences were considered significant when *$P<0.05$ and **$P<0.01$.

Western blotting of phospho-PKA substrates and tyrosine phosphorylation

Immediately after swim-out (T0) and after 60 min of incubation in TYH capacitation medium (T60), proteins from $1×10^6$ sperm were extracted for western blot analysis using Laemmli buffer as previously described (Alvau et al., 2016). Protein extracts were analyzed by SDS-PAGE and electro-transferred to PVDF membranes. Membranes were blocked with 5% fat-free milk in T-TBS (TBS with 0.1% Tween 20) and immunoblotting was conducted with phospho-PKA substrate antibody (1:10,000, Cell Signaling Technology, 9624, clone 100G7). Membranes were washed with T-TBS twice and incubated with HRP-conjugated anti-rabbit secondary antibody (1:10,000 dilution; Fisher Scientific, Cat. No. 45-000-682). Enhanced chemiluminescence (ECL) Plus Kit (Fisher Scientific, Cat. No. RPN2132) was used for detection. After development of pPKAs, PVDF membranes were stripped at 65°C for 20 min in 2% SDS, 0.74% β-mercaptoethanol, 62.5 mM Tris, pH 6.5, and then thoroughly washed with T-TBS. PDVF membranes were then blocked with 5% fish gelatin followed by immunoblotting with anti-pY antibody (1:10,000 dilution; Millipore, Cat No. 05-321, clone 4G10). Membranes were washed with T-TBS twice and incubated with HRP-conjugated anti-mouse secondary antibody (1:10,000; Jackson ImmunoResearch Laboratories, 715-035-150). The ECL Plus Kit was used for detection (Fisher Scientific).

Ca²⁺ imaging

Non-capacitated cauda sperm were used for Ca^{2+} imaging, loaded with 4 μM of the fluorescent Ca^{2+} indicator Fluo-3 AM in the presence of 0.05% pluronic acid at 37°C for 40 min, and protected from light. The cells were washed once, pelleted at 3000 rpm (500 g) for 3 min, and resuspended in TYH media. Sperm were attached onto laminin (1 mg/ml; Invitrogen) precoated cover slips. Fluorescence signals were captured as previously described (Nishigaki et al., 2006), using an inverted microscope (Eclipse TE 300 Nikon) with an oil immersion 60× objective (PlanApo N, numerical aperture 1.42). A LED-based pulsed light excitation system and an iXon888 (512×512 pixels) EMCCD camera (Andor Technology) with 1×1 binning using Andor iQ software were employed in these experiments. Samples were kept at 37°C using a PDMI-2 (Harvard Apparatus) temperature controller. Fluorescence images were captured at 1 frame per second with a 2-ms excitation. For recording, Fluo-3-loaded cells were excited with a cyan LED (3.15 A, Luminus Devices), with a bandpass excitation (HQ 480/40X), dichroic mirror (Q505lp), and emission (HQ 535/ 50 M) filters (Chroma Technology).

Cell culture, transfection and immunoprecipitation

The open reading frames of *C2cd6s*, *Efcab9*, *CatSperζ*, *CatSper2*, *CatSper3* and *CatSper4* were PCR amplified from bulk mouse testis cDNAs. The *CatSper1* open reading frame was amplified from a mouse cDNA clone (MR224271, OriGene). *C2cd6s* was subcloned into pcDNA3.1/myc-His A vector (V800-20, Invitrogen). The others were TA-cloned into pcDNA3.1/V5-His TOPO TA vectors (K4800-01, Invitrogen). HEK293T cells were cultured in DMEM medium with 10% fetal bovine serum in 5% CO_2 at 37°C. Twenty-four to 48 h after transfection with Lipofectamine 2000 (11668-027, Invitrogen), the cells (three wells of a 6-well plate) were lysed in 1 ml IP buffer (50 mM Tris, pH 8.0, 150 mM NaCl, 5 mM $MgCl_2$, 1 mM DTT, 0.5% deoxycholate, 1% Triton X-100) with 1× cocktail of protease inhibitors, incubated at 4°C for 1 h, and centrifuged at 12,000 g for 30 min;

10 μl of supernatant (1%) was set aside as input. The bulk of supernatant (∼1 ml) was incubated with antibodies at 4°C for 1 h: 3 μl (0.5 μg/μl) c-Myc monoclonal antibody (631206, Takara Bio), or 1 μl (1.1 μg/μl) anti-V5 antibody (P/N 46-0705, Invitrogen), or 20 μl anti-C2CD6 (UP2429) antibody. For each immunoprecipitation, 10 μl of Dynabeads G or A (Invitrogen) was added followed by overnight incubation at 4°C. Immunoprecipitated proteins were washed five times with the wash buffer (50 mM Tris, pH 7.5, 250 mM NaCl, 0.1% NP-40, 0.05% deoxycholate) and were eluted in 15 μl 2× SDS sample buffer at 95°C. Elutes and inputs were separated by SDS-PAGE and transferred to nitrocellulose membrane. Anti-c-Myc monoclonal, anti-V5 and anti-CatSper1 (gift from Dejian Ren) (Ren et al., 2001) antibodies were used for western blotting.

References

Alvau, A., Battistone, M. A., Gervasi, M. G., Navarrete, F. A., Xu, X., Sánchez-Cárdenas, C., De la Vega-Beltran, J. L., Da Ros, V. G., Greer, P. A., Darszon, A. et al. (2016). The tyrosine kinase FER is responsible for the capacitation-associated increase in tyrosine phosphorylation in murine sperm. *Development* **143**, 2325-2333. doi:10.1242/dev.136499

Avenarius, M. R., Hildebrand, M. S., Zhang, Y., Meyer, N. C., Smith, L. L. H., Kahrizi, K., Najmabadi, H. and Smith, R. J. H. (2009). Human male infertility caused by mutations in the CATSPER1 channel protein. *Am. J. Hum. Genet.* **84**, 505-510. doi:10.1016/j.ajhg.2009.03.004

Brenker, C., Zhou, Y., Müller, A., Echeverry, F. A., Trötschel, C., Poetsch, A., Xia, X.-M., Bönigk, W., Lingle, C. J., Kaupp, U. B. et al. (2014). The Ca^{2+}-activated K^+ current of human sperm is mediated by Slo3. *eLife* **3**, e01438. doi:10.7554/eLife.01438

Brown, S. G., Miller, M. R., Lishko, P. V., Lester, D. H., Publicover, S. J., Barratt, C. L. R. and Martins Da Silva, S. (2018). Homozygous in-frame deletion in CATSPERE in a man producing spermatozoa with loss of CatSper function and compromised fertilizing capacity. *Hum. Reprod.* **33**, 1812-1816. doi:10.1093/humrep/dey278

Cao, W., Gerton, G. L. and Moss, S. B. (2006). Proteomic profiling of accessory structures from the mouse sperm flagellum. *Mol. Cell. Proteomics* **5**, 801-810. doi:10.1074/mcp.M500322-MCP200

Carlson, A. E., Westenbroek, R. E., Quill, T., Ren, D., Clapham, D. E., Hille, B., Garbers, D. L. and Babcock, D. F. (2003). CatSper1 required for evoked Ca^{2+} entry and control of flagellar function in sperm. *Proc. Natl. Acad. Sci. USA* **100**, 14864-14868. doi:10.1073/pnas.2536658100

Carlson, A. E., Quill, T. A., Westenbroek, R. E., Schuh, S. M., Hille, B. and Babcock, D. F. (2005). Identical phenotypes of CatSper1 and CatSper2 null sperm. *J. Biol. Chem.* **280**, 32238-32244. doi:10.1074/jbc.M501430200

Chang, M. C. (1951). Fertilizing capacity of spermatozoa deposited into the fallopian tubes. *Nature* **168**, 697-698. doi:10.1038/168697b0

Chávez, J. C., Ferreira, J. J., Butler, A., De La Vega Beltrán, J. L., Treviño, C. L., Darszon, A., Salkoff, L. and Santi, C. M. (2014). SLO3 K^+ channels control calcium entry through CATSPER channels in sperm. *J. Biol. Chem.* **289**, 32266-32275. doi:10.1074/jbc.M114.607556

DEVELOPMENT

Chung, J.-J., Navarro, B., Krapivinsky, G., Krapivinsky, L. and Clapham, D. E. (2011). A novel gene required for male fertility and functional CATSPER channel formation in spermatozoa. *Nat. Commun.* **2**, 153. doi:10.1038/ncomms1153

Chung, J.-J., Shim, S.-H., Everley, R. A., Gygi, S. P., Zhuang, X. and Clapham, D. E. (2014). Structurally distinct Ca^{2+} signaling domains of sperm flagella orchestrate tyrosine phosphorylation and motility. *Cell* **157**, 808-822. doi:10.1016/j.cell.2014.02.056

Chung, J.-J., Miki, K., Kim, D., Shim, S.-H., Shi, H. F., Hwang, J. Y., Cai, X., Iseri, Y., Zhuang, X. and Clapham, D. E. (2017). CatSperzeta regulates the structural continuity of sperm Ca^{2+} signaling domains and is required for normal fertility. *eLife* **6**, e23082. doi:10.7554/eLife.23082

Geng, Y., Ferreira, J. J., Dzikunu, V., Butler, A., Lybaert, P., Yuan, P., Magleby, K. L., Salkoff, L. and Santi, C. M. (2017). A genetic variant of the sperm-specific SLO3 K$^+$ channel has altered pH and Ca^{2+} sensitivities. *J. Biol. Chem.* **292**, 8978-8987. doi:10.1074/jbc.M117.776013

Harlow, E. and Lane, D. (1998). *Using Antibodies: A Laboratory Manual*. Cold Spring Harbor: Cold Spring Harbor Laboratory Press.

Hwang, J. Y., Mannowetz, N., Zhang, Y., Everley, R. A., Gygi, S. P., Bewersdorf, J., Lishko, P. V. and Chung, J.-J. (2019). Dual sensing of physiologic pH and calcium by EFCAB9 regulates sperm motility. *Cell* **177**, 1480-1494.e19. doi:10.1016/j.cell.2019.03.047

Hwang, J. Y., Wang, H., Lu, Y., Ikawa, M. and Chung, J.-J. (2021). *C2cd6*-encoded CatSperτ targets sperm calcium channel to Ca^{2+} signaling domains in the flagellar membrane. *bioRxiv*. doi:10.1101/2021.08.16.456347

Jin, J., Jin, N., Zheng, H., Ro, S., Tafolla, D., Sanders, K. M. and Yan, W. (2007). Catsper3 and Catsper4 are essential for sperm hyperactivated motility and male fertility in the mouse. *Biol. Reprod.* **77**, 37-44. doi:10.1095/biolreprod.107.060186

Kirichok, Y., Navarro, B. and Clapham, D. E. (2006). Whole-cell patch-clamp measurements of spermatozoa reveal an alkaline-activated Ca^{2+} channel. *Nature* **439**, 737-740. doi:10.1038/nature04417

Lin, S., Ke, M., Zhang, Y., Yan, Z. and Wu, J. (2021). Structure of a mammalian sperm cation channel complex. *Nature* **595**, 746-750. doi:10.1038/s41586-021-03742-6

Lishko, P. V., Botchkina, I. L., Fedorenko, A. and Kirichok, Y. (2010). Acid extrusion from human spermatozoa is mediated by flagellar voltage-gated proton channel. *Cell* **140**, 327-337. doi:10.1016/j.cell.2009.12.053

Lishko, P. V., Botchkina, I. L. and Kirichok, Y. (2011). Progesterone activates the principal Ca^{2+} channel of human sperm. *Nature* **471**, 387-391. doi:10.1038/nature09767

Liu, J., Xia, J., Cho, K.-H., Clapham, D. E. and Ren, D. (2007). CatSperβ, a novel transmembrane protein in the CatSper channel complex. *J. Biol. Chem.* **282**, 18945-18952. doi:10.1074/jbc.M701083200

Luo, T., Chen, H.-Y., Zou, Q.-X., Wang, T., Cheng, Y.-M., Wang, H.-F., Wang, F., Jin, Z.-L., Chen, Y., Weng, S.-Q. et al. (2019). A novel copy number variation in CATSPER2 causes idiopathic male infertility with normal semen parameters. *Hum. Reprod.* **34**, 414-423. doi:10.1093/humrep/dey377

Luque, G. M., Xu, X., Romarowski, A., Gervasi, M. G., Orta, G., De la Vega-Beltrán, J. L., Stival, C., Gilio, N., Dalotto-Moreno, T., Krapf, D. et al. (2021). Cdc42 localized in the CatSper signaling complex regulates cAMP-dependent pathways in mouse sperm. *FASEB J.* **35**, e21723. doi:10.1096/fj.202002773RR

Miki, K. and Clapham, D. E. (2013). Rheotaxis guides mammalian sperm. *Curr. Biol.* **23**, 443-452. doi:10.1016/j.cub.2013.02.007

Miller, M. R., Mannowetz, N., Iavarone, A. T., Safavi, R., Gracheva, E. O., Smith, J. F., Hill, R. Z., Bautista, D. M., Kirichok, Y. and Lishko, P. V. (2016). Unconventional endocannabinoid signaling governs sperm activation via the sex hormone progesterone. *Science* **352**, 555-559. doi:10.1126/science.aad6887

Nalefski, E. A. and Falke, J. J. (1996). The C2 domain calcium-binding motif: structural and functional diversity. *Protein Sci.* **5**, 2375-2390. doi:10.1002/pro.5560051201

Navarrete, F. A., García-Vázquez, F. A., Alvau, A., Escoffier, J., Krapf, D., Sánchez-Cárdenas, C., Salicioni, A. M., Darzon, A. and Visconti, P. E. (2015). Biphasic role of calcium in mouse sperm capacitation signaling pathways. *J. Cell. Physiol.* **230**, 1758-1769. doi:10.1002/jcp.24873

Navarrete, F. A., Alvau, A., Lee, H. C., Levin, L. R., Buck, J., Leon, P. M.-D., Santi, C. M., Krapf, D., Mager, J., Fissore, R. A. et al. (2016). Transient exposure to calcium ionophore enables in vitro fertilization in sterile mouse models. *Sci. Rep.* **6**, 33589. doi:10.1038/srep33589

Navarrete, F. A., Aguila, L., Martin-Hidalgo, D., Tourzani, D. A., Luque, G. M., Ardestani, G., Garcia-Vazquez, F. A., Levin, L. R., Buck, J., Darzon, A. et al. (2019). Transient sperm starvation improves the outcome of assisted reproductive technologies. *Front. Cell Dev. Biol.* **7**, 262. doi:10.3389/fcell.2019.00262

Nishigaki, T., Wood, C. D., Shiba, K., Baba, S. A. and Darzon, A. (2006). Stroboscopic illumination using light-emitting diodes reduces phototoxicity in fluorescence cell imaging. *BioTechniques* **41**, 191-197. doi:10.2144/000112220

Orta, G., de la Vega-Beltran, J. L., Martín-Hidalgo, D., Santi, C. M., Visconti, P. E. and Darzon, A. (2018). CatSper channels are regulated by protein kinase A. *J. Biol. Chem.* **293**, 16830-16841. doi:10.1074/jbc.RA117.001566

Qi, H., Moran, M. M., Navarro, B., Chong, J. A., Krapivinsky, G., Krapivinsky, L., Kirichok, Y., Ramsey, I. S., Quill, T. A. and Clapham, D. E. (2007). All four CatSper ion channel proteins are required for male fertility and sperm cell hyperactivated motility. *Proc. Natl. Acad. Sci. USA* **104**, 1219-1223. doi:10.1073/pnas.0610286104

Quill, T. A., Sugden, S. A., Rossi, K. L., Doolittle, L. K., Hammer, R. E. and Garbers, D. L. (2003). Hyperactivated sperm motility driven by CatSper2 is required for fertilization. *Proc. Natl. Acad. Sci. USA* **100**, 14869-14874. doi:10.1073/pnas.2136654100

Ren, D., Navarro, B., Perez, G., Jackson, A. C., Hsu, S., Shi, Q., Tilly, J. L. and Clapham, D. E. (2001). A sperm ion channel required for sperm motility and male fertility. *Nature* **413**, 603-609. doi:10.1038/35098027

Rual, J.-F., Venkatesan, K., Hao, T., Hirozane-Kishikawa, T., Dricot, A., Li, N., Berriz, G. F., Gibbons, F. D., Dreze, M., Ayivi-Guedehoussou, N. et al. (2005). Towards a proteome-scale map of the human protein-protein interaction network. *Nature* **437**, 1173-1178. doi:10.1038/nature04209

Sánchez-Cárdenas, C., Romarowski, A., Orta, G., De la Vega-Beltrán, J. L., Martín-Hidalgo, D., Hernández-Cruz, A., Visconti, P. E. and Darzon, A. (2021). Starvation induces an increase in intracellular calcium and potentiates the progesterone-induced mouse sperm acrosome reaction. *FASEB J.* **35**, e21528. doi:10.1096/fj.202100122R

Santi, C. M., Martínez-López, P., de la Vega-Beltrán, J. L., Butler, A., Alisio, A., Darzon, A. and Salkoff, L. (2010). The SLO3 sperm-specific potassium channel plays a vital role in male fertility. *FEBS Lett.* **584**, 1041-1046. doi:10.1016/j.febslet.2010.02.005

Schreiber, M., Wei, A., Yuan, A., Gaut, J., Saito, M. and Salkoff, L. (1998). Slo3, a novel pH-sensitive K$^+$ channel from mammalian spermatocytes. *J. Biol. Chem.* **273**, 3509-3516. doi:10.1074/jbc.273.6.3509

Smith, J. F., Syritsyna, O., Fellous, M., Serres, C., Mannowetz, N., Kirichok, Y. and Lishko, P. V. (2013). Disruption of the principal, progesterone-activated sperm Ca^{2+} channel in a CatSper2-deficient infertile patient. *Proc. Natl. Acad. Sci. USA* **110**, 6823-6828. doi:10.1073/pnas.1216588110

Stauss, C. R., Votta, T. J. and Suarez, S. S. (1995). Sperm motility hyperactivation facilitates penetration of the Hamster Zona Pellucida. *Biol. Reprod.* **53**, 1280-1285. doi:10.1095/biolreprod53.6.1280

Strünker, T., Goodwin, N., Brenker, C., Kashikar, N. D., Weyand, I., Seifert, R. and Kaupp, U. B. (2011). The CatSper channel mediates progesterone-induced Ca^{2+} influx in human sperm. *Nature* **471**, 382-386. doi:10.1038/nature09769

Suarez, S. S. (2016). Mammalian sperm interactions with the female reproductive tract. *Cell Tissue Res.* **363**, 185-194. doi:10.1007/s00441-015-2244-2

Suárez, S. S. and Osman, R. A. (1987). Initiation of hyperactivated flagellar bending in mouse sperm within the female reproductive tract. *Biol. Reprod.* **36**, 1191-1198. doi:10.1095/biolreprod36.5.1191

Tateno, H., Krapf, D., Hino, T., Sanchez-Cardenas, C., Darzon, A., Yanagimachi, R. and Visconti, P. E. (2013). Ca^{2+} Ionophore A23187 can make mouse spermatozoa capable of fertilizing in vitro without activation of cAMP-dependent phosphorylation pathways. *Proc. Natl. Acad. Sci. USA* **110**, 18543-18548. doi:10.1073/pnas.1317113110

Visconti, P. E., Bailey, J. L., Moore, G. D., Pan, D., Olds-Clarke, P. and Kopf, G. S. (1995). Capacitation of mouse spermatozoa. I. Correlation between the capacitation state and protein tyrosine phosphorylation. *Development* **121**, 1129-1137.

Visconti, P. E., Krapf, D., de la Vega-Beltrán, J. L., Acevedo, J. J. and Darzon, A. (2011). Ion channels, phosphorylation and mammalian sperm capacitation. *Asian J. Androl.* **13**, 395-405. doi:10.1038/aja.2010.69

Vishwakarma, P. (1962). The pH and bicarbonate-ion content of the oviduct and uterine fluids. *Fertil. Steril.* **13**, 481-485. doi:10.1016/S0015-0282(16)34633-7

Vyklicka, L. and Lishko, P. V. (2020). Dissecting the signaling pathways involved in the function of sperm flagellum. *Curr. Opin. Cell Biol.* **63**, 154-161. doi:10.1016/j.ceb.2020.01.015

Wang, H., Liu, J., Cho, K.-H. and Ren, D. (2009). A novel, single, transmembrane protein CATSPERG is associated with CATSPER1 channel protein. *Biol. Reprod.* **81**, 539-544. doi:10.1095/biolreprod.109.077107

Wang, H., McGoldrick, L. L. and Chung, J.-J. (2021). Sperm ion channels and transporters in male fertility and infertility. *Nat. Rev. Urol.* **18**, 46-66. doi:10.1038/s41585-020-00390-9

Wennemuth, G., Babcock, D. F. and Hille, B. (2003). Calcium clearance mechanisms of mouse sperm. *J. Gen. Physiol.* **122**, 115-128. doi:10.1085/jgp.200308839

Xia, J. and Ren, D. (2009). The BSA-induced Ca^{2+} influx during sperm capacitation is CATSPER channel-dependent. *Reprod. Biol. Endocrinol.* **7**, 119. doi:10.1186/1477-7827-7-119

Xu, Z., Abbott, A., Kopf, G. S., Schultz, R. M. and Ducibella, T. (1997). Spontaneous activation of ovulated mouse eggs: time-dependent effects on M-phase exit, cortical granule exocytosis, maternal messenger ribonucleic acid recruitment, and inositol 1,4,5-trisphosphate sensitivity. *Biol. Reprod.* **57**, 743-750. doi:10.1095/biolreprod57.4.743

Yang, F., Gell, K., van der Heijden, G. W., Eckardt, S., Leu, N. A., Page, D. C., Benavente, R., Her, C., Höög, C., McLaughlin, K. J. et al. (2008). Meiotic failure

DEVELOPMENT

in male mice lacking an X-linked factor. *Genes Dev.* **22**, 682-691. doi:10.1101/gad.1613608

Yang, F., Silber, S., Leu, N. A., Oates, R. D., Marszalek, J. D., Skaletsky, H., Brown, L. G., Rozen, S., Page, D. C. and Wang, P. J. (2015). TEX11 is mutated in infertile men with azoospermia and regulates genome-wide recombination rates in mouse. *EMBO Mol. Med.* **7**, 1198-1210. doi:10.15252/emmm.201404967

Zeng, X.-H., Yang, C., Kim, S. T., Lingle, C. J. and Xia, X.-M. (2011). Deletion of the Slo3 gene abolishes alkalization-activated K^+ current in mouse spermatozoa. *Proc. Natl. Acad. Sci. USA* **108**, 5879-5884. doi:10.1073/pnas.1100240108

Zhu, D., Dix, D. J. and Eddy, E. M. (1997). HSP70-2 is required for CDC2 kinase activity in meiosis I of mouse spermatocytes. *Development* **124**, 3007-3014. doi:10.1242/dev.124.15.3007

DEVELOPMENT